

## Binary mixtures: Onset of Dufour driven convection

Stefan J. Linz

*Institut für Theoretische Physik, Universität des Saarlandes, D-6600 Saarbrücken, West Germany*

(Received 1 May 1989)

The onset of convection in binary mixtures enclosed between two horizontal, *isothermal* boundaries and driven by an externally applied vertical concentration gradient is investigated. It is shown that *internal* temperature variations, which are driven by the Dufour effect, can have significant influence on the stability boundaries of the quiescent state, depending on the strength of the Dufour coupling.

### I. INTRODUCTION

Convection,<sup>1-4</sup> i.e., the motion of liquids and gases setting in if buoyancy (caused by density differences in the fluid) overcomes internal dissipative effects like viscous friction and diffusion, has recently attracted much interest mainly because convective systems serve as paradigms in bifurcation theory and structure formation. Besides Rayleigh-Bénard convection in pure fluids convection in (chemically nonreacting and miscible) binary mixtures is of growing interest. In that system temperature and concentration are not independent but coupled via the Soret and Dufour effect.<sup>1-4</sup> In the most extensively studied geometry<sup>4</sup> an externally applied temperature gradient is the basic driving for convection: In *liquid* mixtures of alcohol and water and <sup>3</sup>He-<sup>4</sup>He (where the onset of convection is not well understood<sup>5,6</sup>) the Soret effect dominates and the Dufour effect is negligible.<sup>3,7</sup> In gaseous mixtures<sup>7</sup> the Dufour coupling becomes more and more important and can change the stability behavior significantly in comparison to liquid mixtures. Here we present a different setup, in which the Dufour effect is never negligible and plays the dominant role in liquid as well as in gaseous mixtures.

For definitiveness we consider (cf. Fig. 1) a horizontal layer of height  $d$  of a binary mixture, characterized by the mass diffusivity  $D$ , the thermal diffusivity  $\kappa$ , and the kinematic viscosity  $\nu$ , between two parallel, laterally infinite extended, *isothermal*, heat conducting boundaries in the vertically acting gravitational field  $\mathbf{g} = -g\mathbf{e}_z$ . Between the upper boundary, at concentration  $C_0$ , and the

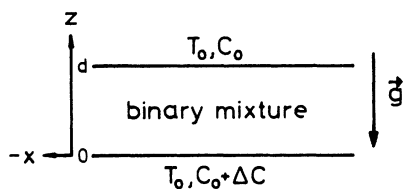


FIG. 1. Binary liquid or gas mixture between lateral infinite extended isothermal boundaries. A concentration gradient externally applied is between the boundaries. The gravitational field  $\mathbf{g}$  acts downwards.

lower boundary, at concentration  $C_0 + \Delta C$ , there is a concentration gradient  $\Delta C$  of arbitrary sign. Solutal expansion creates density differences in the layer which—due to buoyancy—can destabilize the motionless state if  $|\Delta C|$  is large enough. At first sight, there seems to exist a straight similarity to the Rayleigh-Bénard system in a pure fluid, if concentration  $C$ , mass diffusivity  $D$ , and solutal expansion coefficient  $\beta$  of the mixture are substituted by temperature  $T$ , thermal diffusivity  $\kappa$ , and thermal expansion coefficient  $\alpha$  of a pure liquid, respectively. Then one would expect that the motionless state becomes unstable at a fixed critical concentration difference  $\Delta C_{\text{crit}} = a(D\nu/\beta g d^3)$ , where  $a$  depends on the assumed velocity field boundary conditions at the boundaries (for free-slip horizontal boundary conditions,  $a = 27\pi^4/4$ ). All these arguments are based on the assumption that the temperature within the layer is constant, since the plates are at the same temperature  $T_0$ . But in general one has to also allow *internal temperature* variations in the layer since the Dufour effect drives via the diffusive mass-current temperature fluctuations. Then significant changes of the linear and nonlinear behavior can arise in the system. The purpose of this paper is to study in detail the effect of the Dufour-generated internal temperature variations on the stability of the motionless state.

Our paper is organized as follows. In Sec. II we give the underlying equations of velocity, temperature, and concentration. In Sec. III the motionless state is determined. A detailed calculation of the stability boundaries is given in Sec. IV, where also a typical *scenario* for the influence of growing Dufour coupling is presented. The influence of barodiffusion is studied in Sec. V. Section VI contains a comparison of no-slip versus free-slip velocity boundary-condition results for the stability boundaries and a speculation about the strength of the Dufour effect in gases. A summary in Sec. VII closes the paper.

### II. BASIC EQUATIONS

Convection in binary mixtures is described in terms of three field equations for the velocity  $\mathbf{u} = (u, v, w)$ , the temperature  $T$ , and the concentration  $C$ . In the Oberbeck-Boussinesq approximation these equations<sup>1</sup> are

$$(\partial_t + \mathbf{u} \cdot \nabla) \mathbf{u} = -\nabla(p + \hat{g}z) + \mathbf{e}_z \sigma (T - T_0 + C - C_0) + \sigma \nabla^2 \mathbf{u}, \quad (1a)$$

$$(\partial_t + \mathbf{u} \cdot \nabla) T = \nabla^2 T - QL \psi \nabla^2 (C - \psi T), \quad (1b)$$

$$(\partial_t + \mathbf{u} \cdot \nabla) C = L \nabla^2 (C - \psi T), \quad (1c)$$

$$\nabla \cdot \mathbf{u} = 0. \quad (1d)$$

We have scaled length by the layer height  $d$ ; time by  $d^2/\kappa$ ; temperature by  $\kappa\nu/\alpha g d^3$ , where  $\alpha$  is the thermal expansion coefficient of the binary mixture; concentration by  $\kappa\nu/\beta g d^3$ , where  $\beta$  is the solutal expansion coefficient of the mixture; and the quotient of pressure and mass density at the upper boundary  $p$  by  $\kappa^2/d^2$ .  $\hat{g} = g d^3/\kappa^2$  is the dimensionless gravitational acceleration. In addition we have introduced the Prandtl number  $\sigma = \nu/\kappa$ , the Lewis number  $L = D/\kappa$ , and the separation ratio  $\psi$  given by

$$\psi = -\frac{\beta}{\alpha} \frac{k_T}{T_0}, \quad (2a)$$

where  $k_T$  is the thermodiffusion ratio. The index 0 refer to the reference state at the upper boundary. The Dufour number  $Q$  is defined by

$$Q = \frac{T_0 \alpha^2}{c_p \beta^2} \left( \frac{\partial \mu}{\partial \tilde{C}} \right)_{T,p}^0. \quad (2b)$$

Here  $c_p$  is the specific heat at constant pressure and concentration and  $\mu$  the chemical potential of the mixture,<sup>1,2</sup>  $\tilde{C}$  is the unscaled concentration, and  $\tilde{C} = (\kappa\nu/\beta g d^3) C$ . Thus the Dufour number  $Q$  does not depend on the layer height  $d$ . Since  $(\partial \mu / \partial \tilde{C})_{T,p}^0$  is always positive,<sup>1</sup>  $Q$  is also positive. Note that we have ignored in (1) the barodiffusion contribution<sup>2,8</sup> in the diffusive concentration current  $\mathbf{J}_c = -L \nabla (C - \psi T)$ , which will be considered in Sec. V of this paper. Since later on we are only interested in the onset of convection, the assumption of incompressibility,  $\nabla \cdot \mathbf{u} = 0$ , of the mixtures does *not* exclude gaseous mixtures from our discussion.

The Dufour effect, i.e., the coupling of the concentration current in the temperature field equation, is represented by  $-QL \nabla^2 (C - \psi T)$  in (1b).  $QL$  measures the strength of the Dufour effect. For the following it is important that the Dufour effect also contributes to the term proportional to  $\nabla^2 T$ , a fact sometimes overlooked in the literature on binary mixtures (see Ref. 9 for a discussion of that point).

### III. MOTIONLESS STATE

The simplest solution of the field equations (1a)–(1d) is the quiescent or motionless state (index ml) where the *barycentric* velocity  $\mathbf{u}$  is zero everywhere in the layer and the temperature and concentration fields are time independent. Then the two conditions

$$(1 + QL \psi^2) \nabla^2 T_{ml} = QL \psi \nabla^2 C_{ml} \quad (3a)$$

and

$$\nabla^2 C_{ml} = \psi \nabla^2 T_{ml} \quad (3b)$$

from Eqs. (1b) and (1c) can only be fulfilled for nonzero  $Q$ ,  $L$ , and  $\psi$  if  $\nabla^2 C_{ml} = 0 = \nabla^2 T_{ml}$ . Due to the isothermality of the boundaries the temperature in the motionless state is constant everywhere in the layer and equals  $T_0$ . The concentration field varies linearly across the layer height

$$C_{ml}(z) - C_0 = (1 - z) R_s, \quad (4)$$

where the solutal Rayleigh number  $R_s$  is nothing other than the dimensionless concentration gradient  $\Delta C$ ,

$$R_s = \Delta C. \quad (5)$$

Since neither the temperature  $T_0$  nor  $Q$ ,  $L$ , and  $\psi$  enter into the concentration profile of the motionless state, the Dufour effect has no influence on this state, but—as we will see later—on its stability. Finally note that there is a constant vertical concentration current  $\mathbf{J}_c^{ml} = LR_s \mathbf{e}_z$  into the direction of lower concentration, because of our “permeable” concentration boundary condition.

## IV. ONSET OF CONVECTION

### A. Linearized equations

Here we want to determine the solutal Rayleigh number at which, depending on the Lewis number  $L$ , the Prandtl number  $\sigma$ , the separation ratio  $\psi$ , and the Dufour number  $Q$ , convective motion sets in if  $|\Delta C|$  is increased quasistatically. The linearized equations for the deviations from the motionless state,  $\theta = T - T_0$  and  $c = C - C_{ml}(z)$ , of a two dimensional flow  $\mathbf{u} = (u, 0, w)$  are

$$(\partial_t - \sigma \nabla^2) \nabla^2 w = \sigma \partial_x^2 (\theta + c), \quad (6a)$$

$$\partial_t \theta = (1 + QL \psi^2) \nabla^2 \theta - QL \psi \nabla^2 c, \quad (6b)$$

$$\partial_t c = R_s w + L \nabla^2 c - L \psi \nabla^2 \theta. \quad (6c)$$

If one neglects the Dufour effect by setting  $Q = 0$ , the temperature field  $\theta$  relaxes exponentially to zero and the temperature field has no influence on the stability boundaries. Moreover, the special case  $\psi = 0$  has the same effect as setting  $Q = 0$  in (6a)–(6c). Since in general neither the separation ratio  $\psi$  nor the Dufour number  $Q$  vanishes for liquid and gas mixtures temperature fluctuations within the layer will be driven by concentration fluctuations and produce an additional contribution to buoyancy. As long as the internal friction overcomes the buoyancy the motionless state will be stable. To carry out the linear-stability analysis of the motionless state we have to specify the following.

### B. Boundary conditions

As mentioned in the Introduction, an external concentration gradient between the boundaries at  $z = 0$  and 1 is applied in such a way that

$$c(z = 0) = c(z = 1) = 0. \quad (7a)$$

Note that our concentration boundary conditions require “permeability” of the boundaries. Isothermality of the

boundaries implies for the temperature fluctuations

$$\theta(z=0)=\theta(z=1)=0. \quad (7b)$$

Beyond this we assume that the boundaries are well heat conducting, such that heat currents can also flow vertically through the boundaries, i.e.,  $\partial_z \theta \neq 0$  at  $z=0, 1$ , trying to compensate local temperature variations in the layer. Finally we assume free-slip boundary conditions for the velocity field at the boundaries

$$w = \partial_z^2 w = 0 \quad \text{at } z=0, 1. \quad (7c)$$

For these kinds of boundary conditions we are able to perform the stability analysis of the motionless state exactly. More realistic no-slip boundary conditions seem to cause only slight changes, as discussed at the end of the paper.

### C. Appropriate mode expansions for the fields

Since we assume a lateral infinite extended layer (or lateral periodic boundary conditions), we decompose the lateral dependence of the fields in plane waves  $\sim e^{iklx}$  with wave number  $k$  and integer  $l$ . Due to our vertical boundary conditions, see Eqs. (7a)–(7c), one can easily show that for any integer and positive  $n$

$$\partial_z^{2(n+1)} w = \partial_z^{2n} \theta = \partial_z^{2n} c = 0 \quad (7d)$$

at the boundaries  $z=0, 1$ . Therefore  $\{\sqrt{2}\sin(m\pi z), m \text{ integer and positive}\}$  is the appropriate system of orthonormal modes for the vertical dependence of the fields  $w$ ,  $\theta$ , and  $c$ .

### D. Characteristic equation

Standard linear-stability analysis for the motionless state leads to a cubic equation for the characteristic exponent  $\lambda$  governing the temporal behavior of small disturbances from the motionless state:

$$\begin{aligned} & \lambda^3 + q^2[1 + \sigma + L(1 + Q\psi^2)]\lambda^2 \\ & + q^4[L + \sigma + L\sigma(1 + Q\psi^2) - \sigma(k^2/q^6)R_s]\lambda \\ & + \sigma q^6\{L - (k^2/q^6)[1 + QL\psi(1 + \psi)]R_s\} = 0, \end{aligned} \quad (8)$$

where  $q^2 = k^2 + \pi^2$ . For  $\psi=0$  there is a stationary instability ( $\text{Re}\lambda=0$  and  $\text{Im}\lambda=0$ ) at  $R_s(k) = (q^6/k^2)L$ , which has its minimum  $R_s^0 = (27\pi^4/4)L$  at the critical wave number  $k_c^0 = \pi/\sqrt{2}$ . In the following we reduce wave numbers and solutal Rayleigh numbers by their values at  $\psi=0$ ,

$$\hat{k} = k/k_c^0, \quad \hat{q}^2 = q^2/(3\pi^2/2), \quad s = R_s/R_s^0,$$

since this scaling facilitates a comparison with no-slip boundary results (see Sec. V). Note that  $\hat{k}=1$  implies  $\hat{q}=1$ .

### E. Stationary instability

The motionless state becomes unstable towards stationary growth of small internal disturbances at the stationary instability

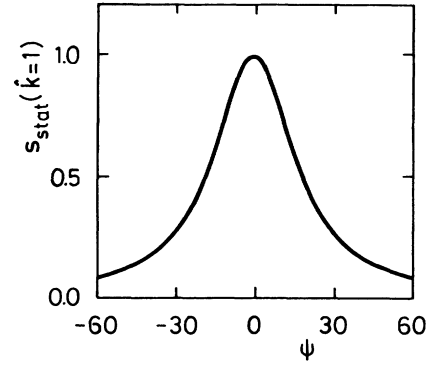


FIG. 2. Critical (stationary) stability boundary of the motionless state  $s_{\text{stat}}(\hat{k}=1)$  as a function of the separation ratio  $\psi$  for a typical liquid mixture (ethanol and water).  $L=0.015$ ,  $\sigma=18.4$ , and  $Q=0.2$ . Ignoring the Dufour effect leads to  $s_{\text{stat}}(\hat{k}=1, Q=0) \equiv 1$ , corresponding to a straight horizontal line in the  $\psi$ - $s$  plane. Only for demonstration purposes such an extended  $\psi$  range is shown.

$$s_{\text{stat}}(\hat{k}) = \frac{\hat{q}^6}{\hat{k}^2} \frac{1}{1 + QL\psi(1 + \psi)}, \quad (9)$$

where the real and imaginary part of  $\lambda$  vanishes.  $s_{\text{stat}}(\hat{k})$  has its critical value at the critical wave number  $\hat{k}_{\text{stat}}^c(\psi)=1$ , which is constant for all  $Q$ ,  $L$ , and  $\psi$ . From Eq. (9) we get the following.

- (i)  $s_{\text{stat}}(\hat{k})$  does not depend on the Prandtl number.
- (ii) In any case for nonzero  $Q$  the stationary instability drops to zero for large positive or negative separation ratios proportional to  $(1/QL)\psi^{-2}$ . In Fig. 2 we show the critical stationary solutal Rayleigh number  $s_{\text{stat}}^c = s_{\text{stat}}(\hat{k}=1)$  as a function of  $\psi$  for  $L=0.015$ ,  $\sigma=18.4$ , and  $Q=0.2$  (values for a ethanol-water mixture<sup>10</sup> at room temperature).

(iii) As long as  $QL < 4$  there is only a stationary instability for positive solutal Rayleigh numbers with its maximum at  $\psi = -\frac{1}{2}$  and fixed to  $s_{\text{stat}}^c = 1$  at  $\psi=0$ . Approaching  $QL=4$  this maximum at  $\psi = -\frac{1}{2}$  diverges,  $s_{\text{stat}}(\psi = -\frac{1}{2}, QL \rightarrow 4) \rightarrow \infty$ .

(iv) For  $QL > 4$  there is a stationary instability for negative solutal Rayleigh numbers in the range  $\psi_{\text{stat},1}^D < \psi < \psi_{\text{stat},2}^D$ , where

$$\psi_{\text{stat},1,2}^D = -\frac{1}{2} [1 \mp \sqrt{(QL-4)/QL}]. \quad (10)$$

At  $\psi_{\text{stat},1}^D$  and  $\psi_{\text{stat},2}^D$ ,  $s_{\text{stat}}$  diverges. Note that a stationary instability for negative solutal Rayleigh numbers can only exist for negative  $\psi$ , with its minimum  $s_{\text{stat}}(\hat{k}=1, \psi = -\frac{1}{2}) = (1 - QL/4)^{-1}$  at  $\psi = -\frac{1}{2}$ .

### F. Oscillatory instability and Hopf frequency

The motionless state becomes unstable towards oscillatory growth of small internal disturbances at the oscillatory instability

$$s_{\text{osc}}(\hat{k}) = \frac{\hat{q}^6}{\hat{k}^2} \frac{[1/L + 1 + Q\psi^2][1 + \sigma + L/\sigma + L(1 + Q\psi^2)]}{\sigma + L(1 - Q\psi)}, \quad (11)$$

in a parameter range in which  $\text{Im}\lambda = \omega_H$  is a real quantity, i.e., when the square of

$$\omega_H^2(\hat{k}) = -\frac{9}{4}\pi^4\hat{q}^4 \frac{[\sigma + L + L\sigma(1 + Q\psi^2)][1 + QL\psi(1 + \psi)] - L\sigma}{\sigma + L(1 - Q\psi)} \quad (12)$$

is positive. As in the stationary case the critical wave number for the growing disturbances is  $\hat{k}_{\text{osc}}^c(\psi) = 1$ . From Eqs. (11) and (12) we get the following.

(i) For large  $|\psi|$   $s_{\text{osc}}$  is proportional to  $-Q\psi^3$  and  $\omega_H^2$  proportional to  $LQ\psi^3$ . Because of this, there is no oscillatory instability for large negative separation ratios.

(ii)  $s_{\text{osc}}$  as well as  $\omega_H^2$  diverge at  $\psi_{\text{osc}}^D = (\sigma + L)/QL$ , which is always positive. For  $\psi > \psi_{\text{osc}}^D$  the denominator of  $s_{\text{osc}}$  and  $\omega_H^2$  is negative. On the other hand the numerator of  $s_{\text{osc}}$  is positive and the numerator of  $\omega_H^2$  is negative whenever  $\psi$  is positive. This implies the existence of an oscillatory for negative solutal Rayleigh numbers if  $\psi > \psi_{\text{osc}}^D$ . This instability is always present if  $Q \neq 0$ , but the corresponding  $s_{\text{osc}}$  value is typically so large that depending on the experimental setup it can overcome the absolute value of the lower bound of  $s$  discussed in Sec. VI of this paper.

(iii) In the range  $0 < \psi < \psi_{\text{osc}}^D$  no oscillatory instability exists, since there  $\omega_H^2$  is negative.

(iv) For positive solutal Rayleigh numbers an oscillatory instability only exists for  $\psi < 0$  and large enough  $QL$ , i.e.,  $QL$  of the order of 4 or larger, as we will see in Sec. IV G.

### G. Changes of the stability boundaries with growing $QL$

Here we want to discuss how the stability boundaries of the motionless state are changed if  $QL$  is enhanced to

values of about 4. As already discussed in the Introduction, ignoring the Dufour effect in our system leads—independent of the separation ratio  $\psi$  of the mixture—to a stationary instability with a critical value  $s_{\text{stat}}^c = s_{\text{stat}}(\hat{k} = 1, Q = 0) = 1$ . For negative solutal Rayleigh numbers no instability exists.

Taking into account the Dufour effect,  $Q \neq 0$ , provides a destabilization of the motionless state for large  $|\psi|$  in comparison with the case without Dufour effect (see, e.g., Fig. 2). This seems to be the first obvious influence of internal temperature fluctuations generated by the Dufour effect.

In Fig. 3 we present as a representative scenario the changes of the stability thresholds for fixed Prandtl number  $\sigma = 1$  and fixed Lewis number  $L = 0.5$  (typical values for gas mixtures). Then we have changed  $Q$  from  $Q = 6$  to  $Q = 10$  in four steps. In Fig. 3(a)–3(d) the stationary instability  $s_{\text{stat}}^c$ , Eq. (9), represented by solid lines and  $s_{\text{osc}}^c$ , Eq. (11), represented by the dashed lines, are shown for  $-1.5 \leq \psi \leq 0.5$ . Within the shaded area the motionless state is linear stable. For  $QL = 3$ , Fig. 3(a), the stability boundaries look similar to the case of very small  $QL$  values, Fig. 2, but the peak height of  $s_{\text{stat}}^c$  is much larger, and  $s_{\text{osc}}^c$  is shifted downwards from large  $s$  values, but there is still no oscillatory instability for positive solutal Rayleigh numbers, since  $\omega_H^2 < 0$  [see Fig. 3(e)]. Note the strong stabilization of the motionless state for separation ratios  $\psi$  of about  $-\frac{1}{2}$  in comparison to the case where the

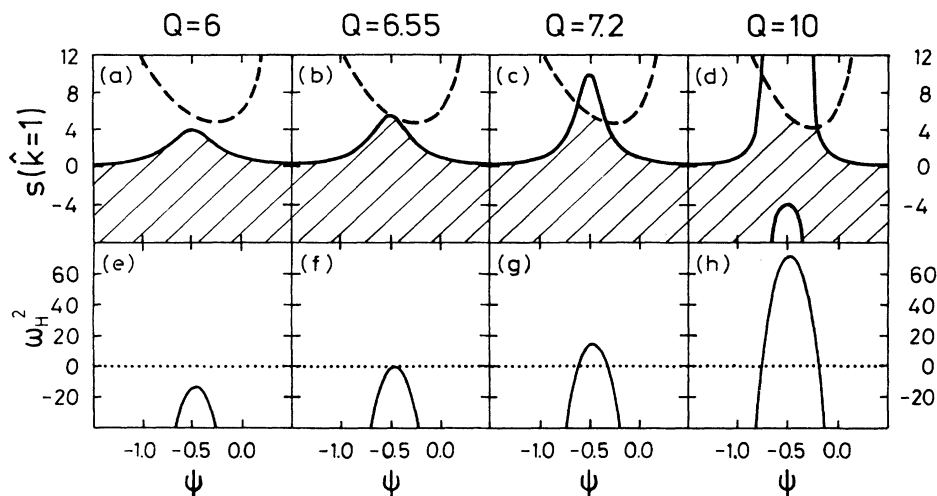


FIG. 3. Critical stability boundaries [(a)–(d)] and square of the Hopf frequency [(e)–(h)] for fixed Prandtl number  $\sigma = 1$  and fixed Lewis number  $L = 0.5$  as function of  $\psi$ . (a) and (e) correspond to  $Q = 6$ , (b) and (f) to  $Q = 6.55$ , (c) and (g) to  $Q = 7.2$ , and (d) and (h) to  $Q = 10$ . In (a)–(d) solid lines represent  $r_{\text{stat}}^c$ , dashed lines represent  $r_{\text{osc}}^c$ . Oscillatory instability only exists if  $\omega_H^2 > 0$ . The shaded area shows the range, where the motionless state is (linear) stable. Above the dotted line in (e)–(h)  $\omega_H^2$  is positive.

Dufour effect is ignored. At  $QL = 3.275$ ,  $s_{\text{osc}}^c$  touches for the first time  $s_{\text{stat}}^c$  and we have the very special case of *one* codimension-two point in the system. Enhancing  $QL$ , e.g., to  $QL = 3.6$ , Figs. 3(c) and 3(g), shifts  $s_{\text{osc}}^c$  further downwards and  $s_{\text{stat}}^c$  is crossed two times by  $s_{\text{osc}}^c$ . Now an oscillatory instability exists between the two crossing points (which are codimension-two points) since the square of the Hopf frequency becomes positive there. Note the typical parabola-shaped form of  $\omega_H^2$ . Up to now no stationary instability for negative  $s$  exists. Enhancing  $QL$  further to values larger than 4 a stationary instability will be evolved for negative solutal Rayleigh numbers  $s < 0$  as shown in Fig. 3(d) where  $QL = 5$ . Further increase of  $QL$  only leads to a “compression” of the stability boundaries, but not to new phenomena. The oscillatory instability for  $s < 0$  is not shown in Fig. 3, since it exists on different  $\omega_H^2$ ,  $s$ , and  $\psi$  scales.

Changing the Prandtl number  $\sigma$  for fixed Lewis number  $L$  and Dufour number  $Q$  only affects the oscillatory instability. For positive solutal Rayleigh and Lewis numbers the oscillatory threshold is essentially shifted downwards (upwards) for  $\sigma > 1$  ( $\sigma < 1$ ) in the  $\psi$ - $s$  plane in comparison with the case  $\sigma = 1$  (cf. Fig. 3): The lower the Prandtl numbers the more stable the motionless state in the  $\psi$  range where an oscillatory instability occurs.

#### H. Codimension-two points

Codimension-two (CT) points,  $\psi_{\text{CT}}(\hat{k})$ , are the points in the  $\psi$ - $s$  plane [see Fig. 3(b)–3(d)], where on the oscillatory instability  $s_{\text{osc}}(\hat{k})$  the Hopf frequency  $\omega_H$  vanishes, i.e.,  $\omega_H^2(\hat{k}, \psi_{\text{CT}}) = 0$ . They coincide with the crossing points of  $s_{\text{osc}}(\hat{k})$  and  $s_{\text{stat}}(\hat{k})$ . First note that if there are CT points, they do not vary with varying wave number  $\hat{k}$ . From Eq. (12) it follows that  $\psi_{\text{CT}}$  is determined by a fourth-order polynomial

$$a\psi_{\text{CT}}^4 + a\psi_{\text{CT}}^3 + (b_1 + b_2)\psi_{\text{CT}}^2 + b_1\psi_{\text{CT}} + b_3 = 0, \quad (13)$$

with

$$\begin{aligned} a &= \sigma Q^2 L^2, \\ b_1 &= (\sigma + L + L\sigma)QL, \\ b_2 &= \sigma QL, \\ b_3 &= \sigma + L. \end{aligned}$$

Since all coefficients of Eq. (13) are positive, CT points (if there are any) are always nonpositive. In the limit  $\sigma \rightarrow 0$ , (13) is reduced to a second-order equation, which shows that two CT points only arise if  $QL > 4$ . For nonzero  $\sigma$  the two CT points begin to exist for somewhat smaller  $QL$ , as can be read off from Fig. 3.

#### V. INFLUENCE OF BARODIFFUSION

Here we want to study the effect of barodiffusion on the onset of convection. Barodiffusion,<sup>2</sup> i.e., the generation of a diffusive concentration current by pressure variations, can be treated easily following Ref. 8 by extending the dimensionless concentration current  $\mathbf{J}_c$ ,

$$\mathbf{J}_c = -L\nabla(C - \psi T) \rightarrow -L\nabla[C - \psi T + (\Gamma/\hat{g})p], \quad (14)$$

by an additional term representing the pressure gradient. The barodiffusion coefficient is given by<sup>8</sup>

$$\Gamma = (g^2 d^4 \beta^2 / \kappa \nu) / (\partial \mu / \partial \tilde{C})_{T,p}. \quad (15)$$

Since  $\Gamma/\hat{g} = g\beta^2 d / \sigma(\partial \mu / \partial \tilde{C})_{T,p}$ , the barodiffusion contribution grows with decreasing Prandtl number. The temperature and the concentration field equation, Eqs. (1b) and (1c), are changed by the incorporation of the barodiffusion term, but the motionless state itself remains *unchanged*. The linearized equations for the deviations from the motionless state read

$$(\partial_t - \sigma \nabla^2) \nabla^2 w = \sigma \partial_x^2 (\theta + c), \quad (16a)$$

$$\begin{aligned} \partial_t \theta &= \{ \nabla^2 + QL \psi [\psi \nabla^2 - \sigma(\Gamma/\hat{g})\partial_z] \} \theta \\ &\quad - QL \psi [\nabla^2 + \sigma(\Gamma/\hat{g})\partial_z] c, \end{aligned} \quad (16b)$$

$$\partial_t c = R_s w + L [\nabla^2 + \sigma(\Gamma/\hat{g})\partial_z] c - L [\psi \nabla^2 - \sigma(\Gamma/\hat{g})\partial_z] \theta. \quad (16c)$$

To eliminate the deviations from the motionless pressure field  $\hat{p}$  we have used

$$\nabla^2 \hat{p} = \sigma \partial_z (\theta + c), \quad (17)$$

which results from the divergence of the velocity field equation (1a). Although first-order derivatives enter into (16b) and (16c) and with it the relation (7d) is no longer valid, the effect of barodiffusion can be estimated,<sup>11</sup> since for typical liquid and gaseous binary mixtures the prefactor  $\Gamma/\hat{g}$  is typically of the order  $10^{-8}$ . Because of that the field expansions used in Sec. IV can be used as trial functions for an approximative linear stability analysis. But after projecting (16a)–(16c) with these trial functions onto  $e^{ikx} \sin \pi z$  the barodiffusion terms drop out. Thus the influence of barodiffusion seems not to be important in our system.

## VI. COMMENTS

### A. No slip boundary conditions

The stability analysis in Sec. IV was carried out with the assumption of free-slip boundary conditions for the vertical velocity field [see Eq. (7c)], since in that case the onset of convection could be determined exactly. This is no longer the case if more realistic no-slip boundary conditions

$$w = \partial_z w = 0 \quad \text{at } z = 0, 1$$

are assumed. Then numerical or approximative Galerkin-like stability analyses have to be performed. In Fig. 4 we show a comparison between our free-slip result and an approximate no-slip result, where the  $w$  field is approximated by the first Chandrasekhar function.<sup>12</sup> Note that in the no-slip case  $R_s^0 \simeq 1728L$  and  $k_c^0 \simeq \pi$ . With these reduction factors, a representative example of  $s(\hat{k} = 1)$  as function of  $\psi$  is shown in Fig. 4. Stationary instabilities cannot be distinguished on this scale. The os-

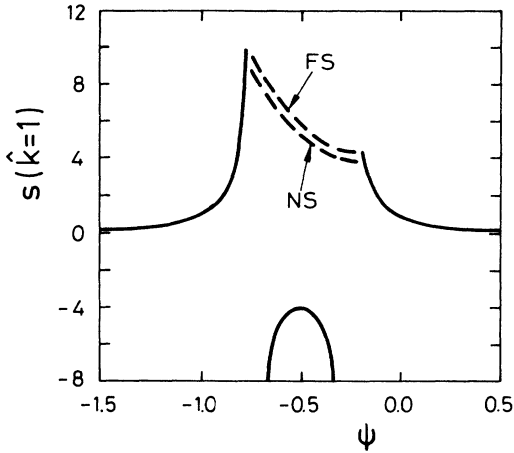


FIG. 4. Comparison between the stability boundaries of the quiescent state for  $L = 0.5$ ,  $\sigma = 1$ , and  $Q = 10$ . Stationary instabilities (solid lines) for free-slip (FS) and approximative no-slip (NS) boundary conditions agree within the pencils width, the oscillatory instabilities (dashed lines) are slightly different.

cillatory instability seems to be shifted a little bit downwards. Because of that the  $\psi$  range for an oscillatory instability is somewhat larger for no-slip boundary conditions. But the scenario presented in Fig. 3 remains not only qualitatively unchanged for no-slip boundary conditions, but also the  $QL$  range where it occurs is nearly the same,  $QL \approx 4$ .

#### B. Upper and lower bound for the solutal Rayleigh number

For the applicability of formula (9) and (11) is essential to keep in mind that the solutal Rayleigh number cannot be varied arbitrarily. Since the unscaled concentration at the lower boundary can only be varied between 0 and 1,

$$0 \leq (\kappa\nu/\beta g d^3)(C_0 + R_s) \leq 1, \quad (18a)$$

for the reduced solutal Rayleigh number the inequality

$$-s_0 \leq s \leq s_m - s_0 \quad (18b)$$

holds (if  $\beta > 0$  is assumed), where  $s_m = \beta g d^3 / \kappa \nu R_s^0$  and  $s_0 = C_0 / R_s^0$ . Obviously the bounds of  $s$  depend on fluid properties ( $\beta, \kappa, \nu$ ), the layer height  $d$ , and the concentration at the upper boundary. The range of accessible  $s$  values grows proportional to  $d^3$  with growing layer height. Due to the different  $R_s^0$  values the range of  $s$  values is smaller for no-slip boundary conditions than for free-slip boundary conditions (by a factor of 0.385).

#### C. Experimental detectability

For small  $QL$  values there is only a decrease of  $s_{\text{stat}}$  to zero for larger  $|\psi|$ . This effect should be detectable in

any binary mixture. But the most interesting new phenomena arise if  $QL$  is of the order of 4. Since in ethanol-water<sup>13</sup> and liquid helium mixtures<sup>13</sup>  $QL$  is of the order of  $10^{-3}$ , in liquid mixtures these new effects are not visible. But gaseous mixtures seem to be a candidate to reach  $QL \approx 0(4)$ , since there the diffusivity  $D = \kappa L$  is typically about 50 000 times larger than in liquids. As an alternative to (2b)  $QL$  is also given by

$$QL = \frac{DT_0\rho_0\alpha^2}{\lambda\beta^2} \left( \frac{\partial\mu}{\partial\tilde{C}} \right)_{p,T}^0, \quad (19)$$

where  $\lambda$  is the heat conductivity and  $\rho_0$  the density of the mixture at the upper boundary. Up to now we have not succeeded in finding tables, where *all* parameters entering (19) are given for different gaseous mixtures, e.g., for mixtures of rare gases. Let us *roughly estimate*  $QL$  by using typical values which can be found in standard tables:<sup>14</sup>  $(\partial\mu/\partial\tilde{C})_{p,T}^0 \approx 10^{+9} \text{ cm}^2/\text{sec}^2$ ,  $\beta \approx 0.5$ ,  $\alpha \approx \frac{1}{273} \text{ K}^{-1}$ ,  $\lambda \approx 10^{-4} \text{ W cm}^{-1} \text{ K}^{-1}$ ,  $D \approx 0.5 \text{ cm}^2/\text{sec}$ , and  $\rho_0 \approx 10^{-3} \text{ g/cm}^3$  (at normal pressure). This leads to an estimate for  $QL$  of the order of 10. Finally, it is noteworthy that  $QL$  can be changed by changing the mean temperature  $T_0$  or by working at different pressure.

#### VII. CONCLUSION

We have discussed the onset of convection in binary mixtures between two horizontal, isothermal boundaries driven by an external, vertical concentration gradient. We have demonstrated the influence of internal temperature variations generated by the Dufour effect on the stability boundaries of the quiescent state. Depending on the strength of the Dufour coupling and the separation ratio stationary *and* oscillatory instabilities exist, if  $QL \gtrsim 4$ . We have speculated about the experimental realizability of such large  $QL$  values: Gas mixtures seem to be an appropriate candidate. The scenario presented in Sec. IV G discussed with the assumption of free-slip boundary conditions for the vertical velocity field holds also for more realistic no-slip boundary conditions. Taking into account barodiffusion seems not to be important in this system. Finally we have shown that there exist lower and upper bounds for the solutal Rayleigh number. Up to now our theory is based on the standard Oberbeck-Boussinesq approximation. Depending on the experimental setup also non-Oberbeck-Boussinesq effects must be taken into account. Despite the fact that the external application of a concentration gradient seems to be a hard experimental problem, we hope that experiments will be performed in the future to study the rich bifurcation behavior of this system.

#### ACKNOWLEDGMENTS

Helpful discussions with Professor M. Lücke are gratefully acknowledged. This work was supported by Deutsche Forschungsgemeinschaft.

- <sup>1</sup>G. Z. Gershuni and E. M. Zhukhovitskii, *Convective Stability of Incompressible Fluids* (Keter, Jerusalem, 1976).
- <sup>2</sup>L. D. Landau and E. M. Lifshitz, *Fluid Dynamics* (Pergamon, New York, 1959).
- <sup>3</sup>J. K. Platten and J. C. Legros, *Convection in Fluids* (Springer, Berlin, 1984).
- <sup>4</sup>R. P. Behringer, *Rev. Mod. Phys.* **57**, 657 (1985).
- <sup>5</sup>S. J. Linz and M. Lücke, *Phys. Rev. A* **35**, 3997 (1987); in *Propagation in Systems Far from Equilibrium*, Vol. 41 of *Springer Series in Synergetics* (Springer, Berlin, 1988), p. 292.
- <sup>6</sup>E. Knobloch and D. R. Moore, *Phys. Rev. A* **37**, 860 (1988); M. C. Cross and K. Kim, *Phys. Rev. A* **37**, 3909 (1988); **38**, 529 (1988).
- <sup>7</sup>W. Hort, S. J. Linz, and M. Lücke (unpublished).
- <sup>8</sup>S. J. Linz and M. Lücke, *Phys. Rev. A* **36**, 3505 (1987).
- <sup>9</sup>G. W. T. Lee, P. Lucas, and A. Tyler, *J. Fluid Mech.* **135**, 235 (1983).
- <sup>10</sup>R. Heinrichs, G. Ahlers, and D. Cannell, *Phys. Rev. A* **35**, 2761 (1987).
- <sup>11</sup>For liquid and gaseous mixtures  $(\partial\mu/\partial\tilde{C})$  can be estimated by assuming *ideal* gas mixtures, see Ref. 2 for details. A typical value is  $(\partial\mu/\partial\tilde{C})_{T,p}^0 \simeq 10^9$  cm<sup>2</sup>/sec<sup>2</sup>, see Ref. 8. Typical Prandtl number are 1 (for gases) up to 20 (water-ethanol mixture). The solutal expansion coefficient is typically of the order  $10^{-1}$ .
- <sup>12</sup>S. Chandrasekhar, *Hydrodynamics and Hydromagnetic Stability* (Dover, New York, 1981); J. Niederländer, Diploma thesis, Universität des Saarlandes, 1987.
- <sup>13</sup>This can be calculated by using estimations of the fluid parameters given in Ref. 8.
- <sup>14</sup>See, e.g., *American Institute of Physics Handbook*, edited by D. E. Gray (McGraw-Hill, New York, 1972). Lacking a value of  $\beta$  in gas mixtures, we used a typical value for liquid mixtures.